



SAKARYA ÜNİVERSİTESİ

# FEN BİLİMLERİ ENSTİTÜSÜ DERGİSİ

Sakarya University Journal of Science  
SAUJS

ISSN 1301-4048 e-ISSN 2147-835X Period Bimonthly Founded 1997 Publisher Sakarya University  
<http://www.saujs.sakarya.edu.tr/>

Title: The Effect of Mg Content on the Physical Properties of ZnO Films Deposited by Ultrasonic Spray Pyrolysis

Authors: Emrah SARICA

Received: 2022-10-17 00:00:00

Accepted: 2023-03-12 00:00:00

Article Type: Research Article

Volume: 27

Issue: 3

Month: June

Year: 2023

Pages: 621-633

How to cite

Emrah SARICA; (2023), The Effect of Mg Content on the Physical Properties of ZnO Films Deposited by Ultrasonic Spray Pyrolysis. Sakarya University Journal of Science, 27(3), 621-633, DOI: 10.16984/saufenbilder.1190168

Access link

<https://dergipark.org.tr/en/pub/saufenbilder/issue/78131/1190168>

New submission to SAUJS

<http://dergipark.gov.tr/journal/1115/submission/start>

## The Effect of Mg Content on the Physical Properties of ZnO Films Deposited by Ultrasonic Spray Pyrolysis

Emrah SARICA \*<sup>1</sup> 

### Abstract

ZnO is a versatile material and tailoring its physical properties to the field of application is technologically crucial. Intentionally doping with a foreign element is the most common and useful method for that. In this presented work, ZnO films doped at different Mg concentrations (0%, 5%, 10%, and 15%) were deposited onto glass substrates by ultrasonic spray pyrolysis in order to investigate the effect of Mg doping. AFM and SEM images captured for the morphological investigations revealed that Mg doping deteriorated the surface of the films. The structural analysis showed that the Mg doping at 5% enhanced the structural properties, but the crystallization level was adversely affected at higher Mg concentrations. Optical band gap and Urbach energies increased from 3.30 eV to 3.45 eV and from 79.5 meV to 119.8 meV, respectively. The lowest electrical resistivity was noted as  $8.72 \times 10^1 \Omega \text{cm}$  for Mg-doped ZnO films at 5%.

**Keywords:** Ultrasonic spray pyrolysis, Mg doping, ZnO thin films, optical properties

### 1. INTRODUCTION

One of the most studied metal oxide semiconductors, ZnO has unique physical properties such as consisting of abundant and non-toxic elements, having n-type electrical conductivity in its nature due to native defects (i.e., oxygen vacancies- $V_o$ , zinc interstitials- $Zn_i$ ), large band gap ( $\sim 3.3$  eV) and high excitonic binding energy ( $\sim 60$  meV) etc., [1]. In particular, the high exciton binding energy along with the wide band gap makes ZnO well-suited for opto-electronic devices such as LEDs [2]. Its high transparency which is another feature of ZnO allows transmitting

light with very low losses and this makes ZnO a favorable material in solar cells as a buffer layer or transparent conductive layer in which the light penetrates through and reaches the active region [3–5]. High carrier mobility along with a wide band gap and high optical transmittance also makes ZnO an important material for thin film transistors to be used in future display technologies such as invisible electronic devices [6–8].

However, these superior properties of ZnO may still be insufficient to achieve more efficient optoelectronic or electronic devices. At this point, the effort to tailor the physical

\* Corresponding author: emrahsarica@baskent.edu.tr (E. SARICA)

<sup>1</sup> Faculty of Engineering, Department of Electrical and Electronics Engineering, Baskent University, 06790, Ankara, Turkey

ORCID: <https://orcid.org/0000-0002-9339-5114>



properties of ZnO by external doping with various elements takes the stage. Substitution of Group III (Al, In, Ga etc.) and Group VII (F, Cl etc.) elements with Zn and O, respectively, increases the free electron concentration and hence n-type conductivity whereas p-type conductivity can be achieved with the substitution of Group II (Li, Na, and K) and Group V (N, P, As, and Sb) elements. However, it should be noted that obtaining p-type ZnO requires quite a laborious effort due to the compensation of acceptors by donor defects such as  $Zn_i$ ,  $V_O$  [9].

Bandgap engineering is another endeavor to get efficient devices. For instance, widening in bandgap of ZnO allows transmittance of light in the short wavelength region and it makes ZnO a preferred material for solar blind UV photodetectors, UV-LEDs etc., [10]. At this point, Mg doping reveals remarkable results due to the fact that the bandgap of MgO (7.8 eV) is quite larger than that of ZnO [11]. Liu et al. reported that doping of Mg into ZnO in nanorod form provides a high potential application in UV photodetectors due to its high UV/visible detection ratio as well as fast rise/fall time [12]. Besides, non-toxic ZnO is considered as novel buffer layer in thin film solar cells, and Mg doping is proposed as an effective way to altering conduction band offset at the buffer/absorber interface [13]. Törndahl et al. experimentally investigated the impact of ALD deposited  $Zn_{1-x}Mg_xO$  buffer layer in Cu(In,Ga)Se<sub>2</sub> solar cells and reported that the increasing Mg content till a certain concentration lead to enhancement in open circuit voltage in CIGS solar cells. They also showed that the conduction band offset at buffer/absorber interface can be tailored for  $x < 0.2$ , effectively [14]. Similarly, Li et al. inserted a  $Zn_{1-x}Mg_xO$  layer between ZnO/Sb<sub>2</sub>Se<sub>3</sub> interface and reported that  $Zn_{1-x}Mg_xO$  layer enables to enhance the efficiency by passivating interfacial defects and reducing recombination loss at the ZnO/Sb<sub>2</sub>Se<sub>3</sub> interface [15]. On the other hand, Mg doping into ZnO is not only useful for adjusting energy band levels, but can also

provide functionality to the ZnO. Islam and Azam experimentally showed that Mg doping into ZnO lattice improves the photocatalytic activity by creating localized electronic states within the band gap. It was explained that the probability of electron-hole recombination diminishes due to these localized states that behave as traps for the electrons in the conduction band and hereby photocatalytic activity is enhanced [16]. Okeke et al., on the other hand, proved that Mg doping into ZnO also allows enhancement in antibacterial properties as well as photocatalytic activity [17].

All these studies reveal that Mg doping gives superior properties to ZnO films. Therefore, this study aims to examine the variation in physical properties of ZnO thin films due to the Mg doping, by ultrasonic spray pyrolysis technique.

## 2. MATERIALS AND METHODS

### 2.1. Deposition of Thin Films

In the first step of thin film deposition, microscope slides used as substrate were ultrasonically cleaned in soapy water, acetone, methanol and deionized (DI) water for 15 min, respectively. Substrates were rinsed under running DI water between two consecutive steps. At the second stage, spray solutions were prepared by mixing of (0.05 M)  $Zn(CH_3COO)_2 \cdot 2H_2O$  and (0.05 M)  $MgCl_2 \cdot 6H_2O$  aqueous solution at certain concentrations of 0, 5, 10 and 15 %v/v. Finally, the prepared spray solution was sprayed by passing through the ultrasonic atomizer which operates at 100 kHz onto pre-heated glass substrates for 25 min by keeping the solution flow rate at 4 ml/min. Temperature of glass substrates was kept at  $425 \pm 5^\circ C$  during the deposition and controlled by using an PID controller equipped with iron-constantan thermocouple. Distance between ultrasonic nozzle and substrate was maintained at 30 cm. Compressed air at 0.7 bar pressure was used as carrier gas.

## 2.2. Characterization of Thin Films

Surface morphologies of undoped and Mg-doped ZnO thin films were evaluated by means of atomic force microscope (AFM) and scanning electron microscope (SEM) images. AFM images were captured by Park Systems XE-100 and surface roughness values were determined via XEI version 1.7.1 software. HITACHI SU5000 Field Emission Scanning Electron Microscope was used to get both top surface images and cross-sectional view to determine the film thickness. In addition to that, elemental compositions of all films were confirmed by means of energy-dispersive X-ray spectroscopy (EDS) spectra taken by the Oxford X-MaxN 80 detector which is an attachment of SEM system. Structural investigations of all deposited thin films were carried out by means of X-ray diffraction pattern taken by x-ray diffractometer (PANalytical Empyrean), having  $\text{CuK}\alpha$  radiation ( $\lambda = 1.5406 \text{ \AA}$ ) operating at 40 mA and 45 kV. A continuous scan mode was used to collect  $2\theta$  data from  $25^\circ$  to  $65^\circ$  with a step of  $\Delta(2\theta) = 0.013^\circ$ . Optical transmittance and absorbance spectra belonging to deposited films were recorded by Rigol Ultra-3660 double beam UV-Visible spectrophotometer.

## 3. RESULTS AND DISCUSSIONS

### 3.1. Morphological and Elemental Investigations

Figure 1 shows the 3D-AFM images of undoped and Mg-doped ZnO thin films. Bright and dark regions throughout the surfaces are related to the hill and valley formations, respectively. It indicates the presence of randomly distributed particle formations with different sizes on the surface. Although the ultrasonic nozzle used to spray the prepared solution in fine droplets enables to get droplets of most frequently  $20 \mu\text{m}$  in diameter, the size of the droplets obtained varies in the range of  $10\text{-}60 \mu\text{m}$ . This leads to

formation of hill and valley along the surface of thin films and inhibits to get perfectly smooth surfaces. Average ( $R_a$ ) and root mean square ( $R_q$ ) values of surface roughness of all films were found to be in the range of  $2.02\text{-}4.39 \text{ nm}$  and  $2.69\text{-}5.68 \text{ nm}$ , respectively, and listed in Table 1.

As seen from the Table 1, lowest surface roughness was obtained for undoped ZnO films and roughness increased due to Mg doping. This deterioration in the surface morphologies is also clearly seen in the SEM images given in Figure 2. As seen from Figure 2, undoped ZnO films consisted of grains with a certain geometry but the grain-like appearance disappeared for the Mg-doped films, gradually. This may also be correlated with the deterioration of the crystal structure, as will be discussed later.

Meanwhile, the cross-sectional SEM images were inserted in Figure 2. Film thicknesses were determined as the average of measurements taken from ten different regions along these images via ImageJ software. Thickness of the films were also listed in Table 1.

Figure 3 represents the EDS spectra taken for the compositional analysis of ZnO:Mg thin films. As seen from these spectra strong signals were detected belonging to Zn and O atoms for all films and whereas Mg signal existed for only Mg-doped ZnO films as expected. Besides the Zn, O and Mg signal, a C peak observed for all films it may have come out as surface contamination or environmental impurity. Detected atomic percentage of Mg is noted as 2.4%, 3.6% and 5.7% for Mg doped ZnO at 5%, 10% and 15% v/v, respectively. Although the Mg ratio in EDS spectra was not exactly the same as the ratio in the spray solution, the detected Mg atomic percent in EDS spectra increased as the manganese ratio in the solution increased.

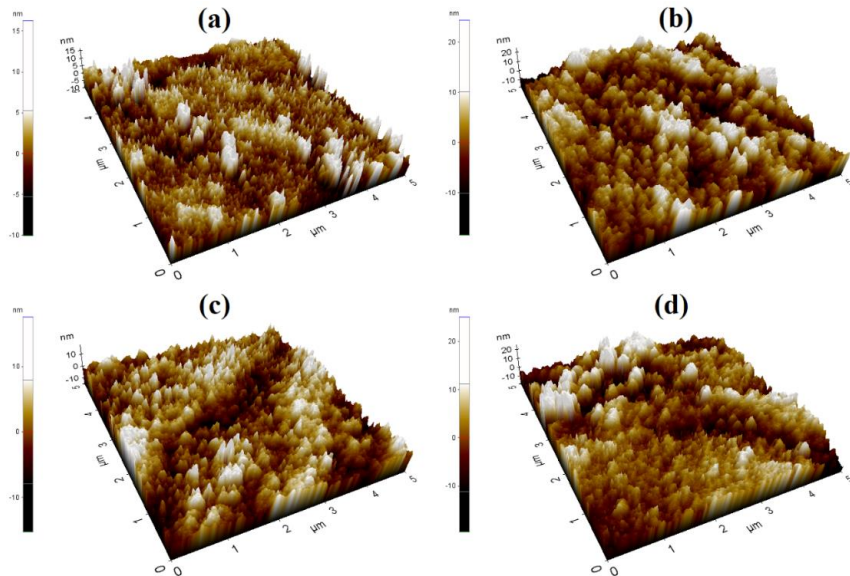


Figure 1 AFM images of (a) undoped and (b) Mg doped at 5% (c) Mg doped at 10% and (d) Mg doped at 15% ZnO thin films

Table 1 Thickness and surface roughness ( $R_a$  and  $R_q$  are the average and root mean square values of roughness) values of all deposited thin films

Material	Thickness (nm)	$R_a$ (nm)	$R_q$ (nm)
ZnO	300	2.02	2.69
ZnO:Mg(5%)	305	4.04	5.16
ZnO:Mg(10%)	205	3.24	4.05
ZnO:Mg(15%)	340	4.39	5.68

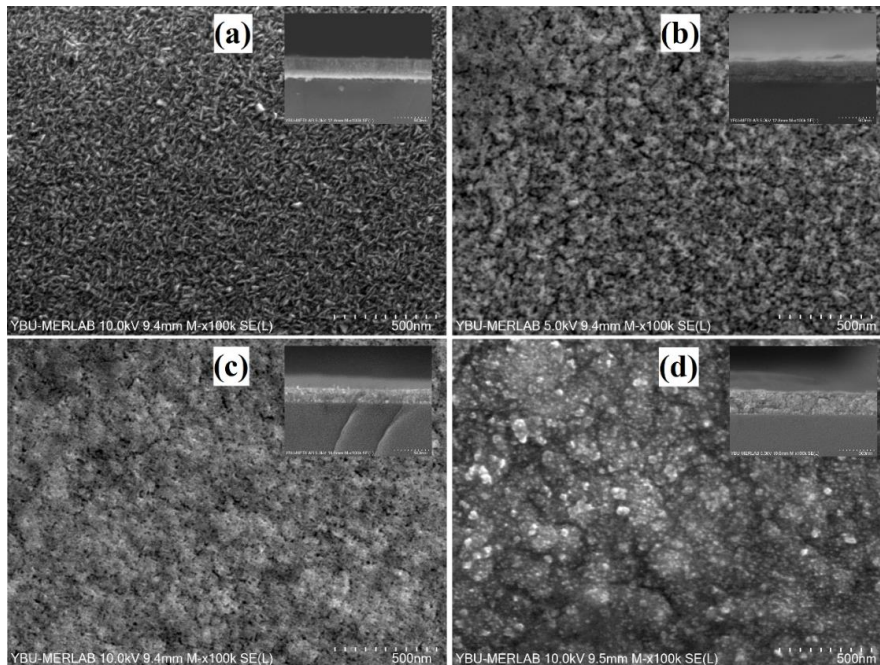


Figure 2 100K magnified surface and cross-sectional (inserted) SEM images of (a) undoped and (b) Mg doped at 5% (c) Mg doped at 10% and (d) Mg doped at 15% ZnO thin films

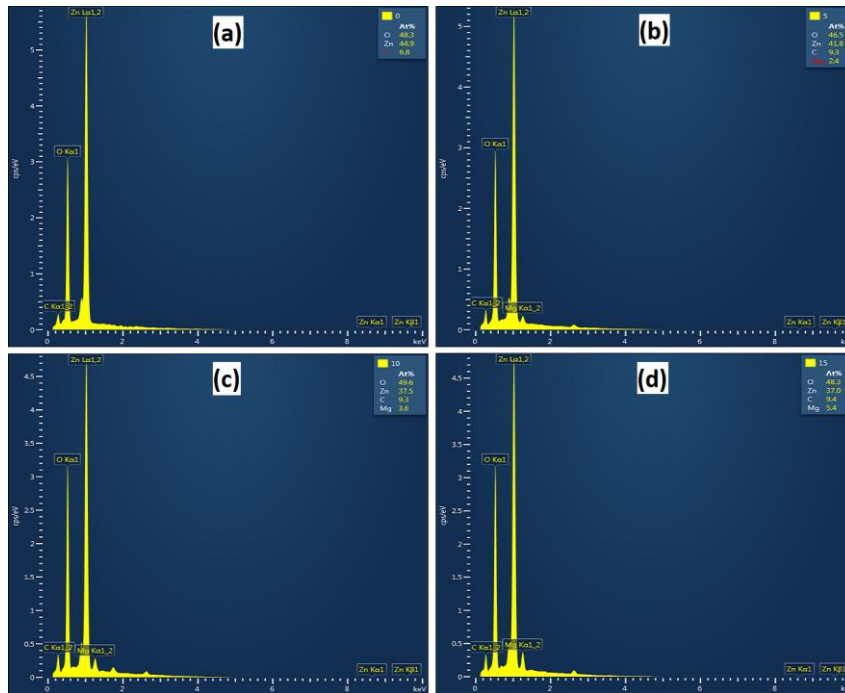


Figure 3 EDS spectra of (a) undoped and (b) Mg doped at 5% (c) Mg doped at 10% and (d) Mg doped at 15% ZnO thin films

### 3.2. Structural Investigations

Structural analysis of ZnO:Mg films were performed by using XRD patterns given in Figure 4. Three diffraction peaks on these patterns located at  $2\theta \approx 32.1^\circ$ ,  $34.8^\circ$  and  $36.6^\circ$  were observed and indexed to (100), (002) and (101) planes of hexagonal ZnO by comparing with PDF 00-036-1451 reference card. However, Mg-related peaks did not exist and it implies that there was no any secondary phase of  $Mg_xO_y$  or ZnMgO. Some structural parameters extracted from the peaks on XRD patterns were listed in Table 2. The intensity of (100) plane peak was found to be higher than peaks of other planes for undoped ZnO films, but it decreased gradually with Mg content. Moreover, full width half maximum (FWHM) values of all peaks exist on XRD patterns increased, except for (200) plane of Mg doped ZnO at 5%. All these indicate that the crystallinity of ZnO films deteriorated by Mg doping.

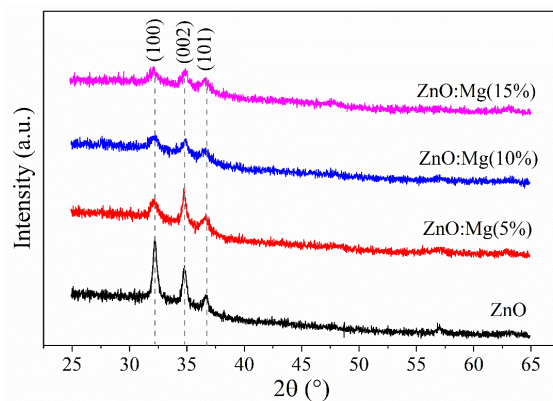


Figure 4 XRD patterns of undoped and Mg doped ZnO thin films

Diffraction angle ( $2\theta$ ) and FWHM ( $\beta$ ) are determinative on the structural parameters of films. Therefore, by using these extracted parameters, lattice constants ( $a$  and  $c$ ), unit volume cell ( $V$ ), mean crystallite size ( $D$ ), and micro-strains were calculated by using the following relations and listed in Table 2.

Lattice constants ( $a$  and  $c$ ) were calculated by following equation [18]

$$\frac{1}{d_{(hkl)}^2} = \frac{4}{3} \left( \frac{h^2 + hk + k^2}{a^2} \right) + \frac{l^2}{c^2} \quad (1)$$

where  $(hkl)$  and  $d$  are the miller indices and interplanar distance  $(d = \lambda / 2 \sin \theta)$ , respectively. Unit cell for hexagonal crystal structure [18];

$$V = \frac{\sqrt{3}}{2} a^2 c \quad \rho = 1 / (qn\mu) \quad (2)$$

Mean crystallite size was calculated by using well-known Scherrer's equation [18]

$$D = \frac{K\lambda}{\beta_{hkl} \cos \theta} \quad (3)$$

where  $K$  is shape factor (0.94),  $\lambda$  is the wavelength of x-ray ( $\lambda_{CuK\alpha} = 0.154$  nm),  $\theta$  is

the Bragg angle. Micro-strain ( $\varepsilon$ ) values were calculated by using following equation [18]

$$\varepsilon = \beta / 4 \tan \theta \quad (4)$$

Based on these calculations it can be concluded that Mg doping adversely affected the crystalline level of ZnO thin films. This may be due to slight differences between ionic radii of  $Zn^{2+}$  ( $\sim 0.74$  Å) and  $Mg^{2+}$  ( $\sim 0.71$  Å) which are also known as crystal radii described as the physical size of ions in a solid by Shannon R.D [19]. Moreover, Mg may have also prevented the formation of ZnO as reported by others [20–22].

Table 2 Peaks position ( $2\theta$ ) FWHM ( $\beta$ ), interplanar spacing ( $d$ ), miller indices ( $hkl$ ),  $a$ -lattice and  $c$ -lattice,  $c/a$  ratio, unit cell volume ( $V$ ), crystallite size ( $D$ ) and micro-strain values ( $\varepsilon$ )

$2\theta$ (°)	$\beta$ (°)	$d$ (Å)	$(hkl)$	$D$ (Å)	$\varepsilon \times 10^{-3}$	$a$ (Å)	$c$ (Å)	$c/a$	$V$ (Å <sup>3</sup> )
32.22	0.4131	2.7764	100	209	6.24				
34.78	0.4515	2.5776	002	193	6.29	3.2059	5.1553	1.608	45.89
36.70	0.4312	2.4471	101	203	5.67				
32.14	0.7632	2.7825	100	113	11.6				
34.77	0.3643	2.5779	002	239	5.08	3.2130	5.1557	1.605	46.09
36.61	0.6891	2.4524	101	127	9.09				
32.14	0.7566	2.7824	100	114	11.5				
34.84	0.5696	2.5727	002	153	7.92	3.2128	5.1454	1.602	45.99
36.58	0.6769	2.4547	101	129	8.94				
32.05	0.8284	2.7901	100	104	12.6				
34.83	0.6251	2.5740	002	139	8.70	3.2218	5.1480	1.598	46.28
36.57	0.7838	2.4554	101	111	10.4				

### 3.3. Optical Investigations

Optical properties were evaluated by means of transmittance and absorbance spectra given in Figure 5(a) and (b), respectively. Figure 5(a) shows that all films exhibit high transparency ( $>90\%$ ) in the visible range of the electromagnetic spectrum and no considerable variation was observed along with the Mg doping. On the other hand, the absorption edge emerged in the range of 325–390 nm as seen from Figure 5(b) and shifted towards shorter wavelength with the Mg doping as clearly seen from the plot given as inset in Figure 5(b). In addition to that, the

absorption edge began to become more oblique with the addition of Mg. These indicate that band gap of deposited films enlarged and band tail fluctuation increased with Mg doping.

In order to determine the band gap of all deposited thin films, extrapolation of the linear portion of the plots of  $(\alpha hv)^2$  vs.  $hv$  at  $(\alpha hv)^2 = 0$  was used according to Tauc's method given by Eq (5), and listed in Table 3.

$$(\alpha hv)^n = A(hv - E_g) \quad (5)$$

where  $h$  is the Planck's constant,  $\nu$  is frequency,  $n$  is equal to 2 for allowed direct transition,  $A$  is a constant and  $E_g$  is the optical band gap. As seen from Table 3, band gap increased from 3.30 eV to 3.45 eV along with the Mg doping. These values are consistent with the previously reported studies and increment in band gap with increasing amount of doped Mg also reported by others [23–27]. In fact, in some reported studies [16, 28–31], the increase in the band gap is higher than this work. Mostly, the enlargement in band gap is attributed to Burstein-Moss effect [16, 25, 26, 30, 32, 33]. Besides, Etacheri et al. state that another important factor affecting the band gap of the semiconductors is the lattice parameter, and an increase in the band gap values is observed along with the decrease of the  $c/a$  ratio [33]. Also, the electronegativity between Zn and Mg has also been suggested as the reason for the band gap widening [24, 28]. In addition to these, a wider band gap of MgO (~7.8 eV) has compared to ZnO may also be the reason for the increase in the band gap in the Mg doped ZnO films [20, 34, 35]. In this study, as will be discussed in the electrical analysis section, there were no

findings that shows a remarkable improvement in electrical properties that could indicate an increase in carrier concentration with the incorporation of Mg. For this reason, it is very hard to explain the enlargement in the band gap seen in this study by the Burstein-Moss effect. So, the enlargement in the band gap might be related to the fact that MgO has a wider bandgap than ZnO. In order to investigate band tail fluctuations,  $\ln\alpha$  vs.  $h\nu$  plots given in Figure 5(d) were constructed and Urbach energy ( $E_u$ ) values for all films extracted from the slope of linear portion according to Eq. (6) and listed in Table 3.

$$\alpha = \alpha_0 \exp\left(\frac{h\nu}{E_u}\right) \quad (6)$$

where  $\alpha_0$  is a constant. As seen from Table 3, Mg doping into ZnO led to increase in  $E_u$  from 79.5 meV to 119.8 meV. This implies that the degree of electronic disorder increases by Mg doping, in another words, the width of the localized states within the forbidden gap increases. Structural disorders such as crystal defects contributes to band tail states and increases the Urbach energy [16, 36].

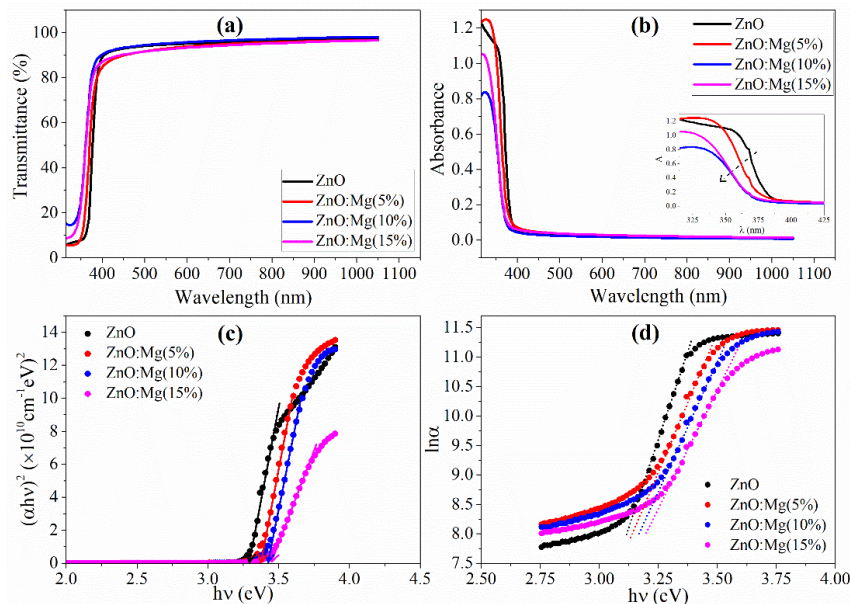


Figure 5 (a) Transmittance (b) absorbance, (c)  $\alpha h\nu-h\nu$  plots, (d)  $\ln\alpha-h\nu$  plots of undoped and Mg doped ZnO thin films

Table 3 Band gap ( $E_g$ ), Urbach energy ( $E_u$ ) and resistivity ( $\rho$ ) values of ZnO:Mg thin films

Material	$E_g$ (eV)	$E_u$ (meV)	$\rho$ ( $\Omega\text{cm}$ )
ZnO	3.30	79.5	$1.57 \times 10^2$
ZnO:Mg(5%)	3.38	102.8	$8.72 \times 10^1$
ZnO:Mg(10%)	3.42	106.9	$4.33 \times 10^2$
ZnO:Mg(15%)	3.45	119.8	$3.05 \times 10^4$

The increase in Urbach energies is also correlated with the deterioration in the crystallization levels of the ZnO:Mg thin films deposited in this work. Similar deviation in the Urbach energies of ZnO with the Mg doping were also reported by Islam and Azam [16]. On the other hand, it is known that band tails tend to reduce the energy band gap of thin films [37, 38]. Therefore, in this work, observed increase in the width of band tails may have suppressed the enlargement in bandgap with Mg doping and inhibited getting larger band gaps.

### 3.4. Electrical Investigations

Electrical investigations were carried out in two steps. In the first step electrical conductivity type was determined by hot point probe techniques and it was noted that all films have n-type conductivity. It is very well known that point defects (i.e., donor defects such as O vacancies and Zn interstitials) are the reason for the n-type conductivity nature in ZnO films.

In the second step electrical resistivity values were measured by means of four-point probe technique at room temperature listed in Table 3. As seen from Table 3, electrical resistivity of Mg doped ZnO at 5% is found to be less than that of the undoped film. However, Mg doping at 10% and 15% led to increasing the electrical resistivity, and it was even found to be higher than the undoped ZnO films. As known, electrical resistivity is related to carrier mobility and carrier concentration according to  $\rho = 1/(qn\mu)$ . It is reported that carrier concentration increases by formation of oxygen vacancies through the Mg doping due to the difference of electronegativity between Mg and Zn [33, 39]. Meanwhile,

increased oxygen vacancy concentration also means a decrease in mobility [40]. Besides, Caglar et. al have stated that the substitution of  $\text{Mg}^{2+}$  and  $\text{Zn}^{2+}$  does not yield extra free electrons because of their equivalent valence state while the interstitial Mg ions donate extra electrons [41]. On the other hand, carrier mobility is directly dependent on the scattering of free carriers, and these scatterings implicitly depend on retardation by hopping transport, phonon scattering, impurity scattering, and grain boundary scattering [42, 43]. High carrier concentration can be achieved with externally doping, but this restricts carrier mobility because it will result in a high amount of ionized impurity and hence impurity scattering [43–45]. Grain boundary scattering, one of the primary carrier scattering mechanisms, is directly linked with the crystallite size as crystallites with small size results in a higher amount of grain boundaries, namely, a higher possibility of grain boundary scattering. Beyond that, segregation of excess Mg ions at the grain boundaries gives rise to an electrical barrier and thus enhances the effectiveness scattering of the carriers [39]. Vinoth et al. also reported that the electrical resistance increased with the decrease of mobility in Mg-doped ZnO films [46].

In fact, the trend in electrical resistivity variations in this work is in harmony with the variation of crystallite size of the films, which can be associated with grain boundary scattering. It can be argued that less electrical resistivity for 5% Mg-doped films compared to that of the undoped film may have been due to the enhancement in crystallite size along with the increase in carrier concentration resulting from the Mg incorporation. However, the relatively high Mg concentration (10% and 15 % v/v) in the spray

solution may have caused Mg segregation at the grain boundaries which may have resulted in grain boundary scattering more effective. Therefore, increase in the resistivity of 10% and 15% Mg-doped films may have been predominantly related to carrier mobility suffering grain boundary scattering. Additionally, as given in the optical analysis section, the increase in Urbach energies indicates the increase in localized states that act as traps for charge carriers [16]. This may be another reason for the rise in electrical resistivity.

#### 4. CONCLUSION

In this work, Mg-doped ZnO thin films were successfully deposited onto glass substrates without any crack or void along the surface. However, the increase in surface roughness with Mg doping indicates that the morphology deteriorated. In addition to that, high amount of Mg doping led to not only a decrease in x-ray diffraction peak intensity but also a broadening of them which indicates shrinkage in crystallite size. Therefore, it can be concluded that Mg doping at these ratios has adversely affected both the crystallization and morphology of ZnO thin films.

In terms of optical properties, it was found that Mg doping is convenient to get a ZnO film with a larger bandgap, whereas it causes an increase in localized defects within the band gap and band fluctuations considering the increase in Urbach energies. In addition to these, it was determined that electrical conductivity can be enhanced by Mg doping at 5%, but further doping concentrations caused a decrease in conductivity, due to the possibility of increased scattering mechanisms.

In order to enhance the crystallization level of Mg doped ZnO films post-annealing treatment can be applied. This may also allow for an increase in the electrical conductivity by reducing free carrier scattering with the enhancement in crystallization level. On the other hand, enhancement in crystallization

level (i.e., reduction in point defects) may also make it possible to obtain a wider band gap by reducing the tailing of the band edges.

#### *Authors' Contribution*

The author confirms sole responsibility for all section of the manuscript.

#### *The Declaration of Conflict of Interest/ Common Interest*

No conflict of interest or common interest has been declared by the author.

#### *The Declaration of Ethics Committee Approval*

This study does not require ethics committee permission or any special permission.

#### *The Declaration of Research and Publication Ethics*

The author of the paper declare that he complies with the scientific, ethical and quotation rules of SAUJS in all processes of the paper and that he does not make any falsification on the data collected. In addition, he declares that Sakarya University Journal of Science and its editorial board have no responsibility for any ethical violations that may be encountered, and that this study has not been evaluated in any academic publication environment other than Sakarya University Journal of Science.

#### REFERENCES

- [1] H. Morkoç, Ü. Özgür, Zinc Oxide: Fundamentals, Materials and Device Technology, Weinheim: Wiley-VCH, 2008.
- [2] J. C. Fan, S. L. Chang, Z. Xie, "ZnO-Based Light-Emitting Diodes," in Optoelectronics - Advanced Materials and Devices, London: IntechOpen, 2013.
- [3] M. A. Martínez, J. Herrero, M. T. Gutiérrez, "Deposition of transparent and conductive Al-doped ZnO thin

- films for photovoltaic solar cells,” *Solar Energy Materials and Solar Cells*, vol. 45, no. 1, pp. 75–86, 1997.
- [4] Y. Lare, A. Godoy, L. Cattin, K. Jondo, T. Abachi, F. R. Diaz, M. Morsli, K. Napo, M. A. del Valle, J. C. Bernède., “ZnO thin films fabricated by chemical bath deposition, used as buffer layer in organic solar cells,” *Applied Surface Science*, vol. 255, no. 13–14, pp. 6615–6619, 2009.
- [5] X. Wen, Y. He, C. Chen, X. Liu, L. Wang, B. Yang M. Leng, H. Song, K. Zeng, D. Li, K. Li, L. Gao, J. Tang, “Magnetron sputtered ZnO buffer layer for Sb<sub>2</sub>Se<sub>3</sub> thin film solar cells,” *Solar Energy Materials and Solar Cells*, vol. 172, pp. 74–81, 2017.
- [6] J. H. Lee, C. H. Ahn, S. Hwang, C. H. Woo, J. S. Park, H. K. Cho, J. Y. Lee, “Role of the crystallinity of ZnO films in the electrical properties of bottom-gate thin film transistors,” *Thin Solid Films*, vol. 519, no. 20, pp. 6801–6805, 2011.
- [7] M. Kumar, H. Jeong, A. Kumar, B. P. Singh, D. Lee, “Magnetron-sputtered high performance Y-doped ZnO thin film transistors fabricated at room temperature,” *Materials Science in Semiconductor Processing*, vol. 71, pp. 204–208, 2017.
- [8] Z. Xiaming, W. Huizhen, W. Shuangjiang, Z. Yingying, C. Chunfeng, S. Jianxiao, Y. Zijian, D. Xiaoyang, D. Shurong, “Optical and electrical properties of N-doped ZnO and fabrication of thin-film transistors,” *Journal of Semiconductors*, vol. 30, no. 3, pp. 033001, 2009.
- [9] Y. S. Choi, J. W. Kang, D. K. Hwang, S. J. Park, “Recent Advances in ZnO-Based Light-Emitting Diodes,” *Ieee Transactions On Electron Devices*, vol. 57, no. 1, pp. 26–41, 2010.
- [10] M. N. H. Mia, M. F. Pervez, M. K. Hossain, M. R. Rahman. M. J. Uddin, M. A. Al Mashud, H.K. Ghosh, M. Hoq, “Influence of Mg content on tailoring optical bandgap of Mg-doped ZnO thin film prepared by sol-gel method,” *Results in Physics*, vol. 7, pp. 2683–2691, 2017.
- [11] P. Giri, P. Chakrabarti, “Effect of Mg doping in ZnO buffer layer on ZnO thin film devices for electronic applications,” *Superlattices and Microstructures*, vol. 93, pp. 248–260, 2016.
- [12] Y. H. Liu, S. J. Young, C. H. Hsiao, L. W. Ji, T. H. Meen, W. Water, S. J. Chang, “Visible-Blind Photodetectors With Mg-Doped ZnO Nanorods,” *IEEE Photonics Technology Letters*, vol. 26, no. 7, pp. 645–648, 2014.
- [13] X. He, L. Wu, X. Hao, J. Zhang, C. Li, W. Wang, L. Feng, Z. Du, “The Band Structures of Zn<sub>1-x</sub>Mg<sub>x</sub>O(In) and the Simulation of CdTe Solar Cells with a Zn<sub>1-x</sub>Mg<sub>x</sub>O(In) Window Layer by SCAPS,” *Energies*, vol. 12, no. 2, pp. 291, 2019.
- [14] T. Törndahl, C. Platzer-Björkman, J. Kessler, M. Edoff, “Atomic layer deposition of Zn<sub>1-x</sub>Mg<sub>x</sub>O buffer layers for Cu(In,Ga)Se<sub>2</sub> solar cells,” *Progress in Photovoltaics: Research and Applications*, vol. 15, no. 3, pp. 225–235, 2007.
- [15] K. Li, K. Li, R. Kondrotas, C. Chen, S. Lu, X. Wen, D. Li, J. Luo, Y. Zhao, J. Tang, “Improved efficiency by insertion of Zn<sub>1-x</sub>Mg<sub>x</sub>O through sol-gel method in ZnO/Sb<sub>2</sub>Se<sub>3</sub> solar cell,” *Solar Energy*, vol. 167, pp. 10–17, 2018.
- [16] M. R. Islam, M. G. Azam, “Enhanced photocatalytic activity of Mg-doped

- ZnO thin films prepared by sol–gel method,” *Surface Engineering*, vol. 37, no. 6, pp. 775–783, 2021.
- [17] I. S. Okeke, K. K. Agwu, A. A. Ubachukwu, I. G. Madiba, M. Maaza, G. M. Whyte, F. I. Ezema, “Impact of particle size and surface defects on antibacterial and photocatalytic activities of undoped and Mg-doped ZnO nanoparticles, biosynthesized using one-step simple process,” *Vacuum*, vol. 187, pp. 110110, 2021.
- [18] B. D. Cullity, *Elements of X-ray Diffraction*, Massachusetts: Addison-Wesley Publishing Company, Inc, 1956.
- [19] R. D. Shannon, “Revised effective ionic radii and systematic studies of interatomic distances in halides and chalcogenides,” *Acta Crystallographica Section A*, vol. 32, no. 5, pp. 751–767, 1976.
- [20] A. Mahroug, B. Mari, M. Mollar, I. Boudjadar, L. Guerbous, A. Henni, N. Selmi, “Studies On Structural, Surface Morphological, Optical, Luminescence and Uv Photodetection Properties Of Sol–Gel Mg-Doped ZnO Thin Films,” *Surface Review and Letters*, vol. 26, no. 03, pp. 1850167, 2019.
- [21] Ş. Tãlu, S. Boudour, I. Bouchama, B. Astinchap, H. Ghanbaripour, M. S. Akhtar, S. Zahra, “Multifractal analysis of Mg-doped ZnO thin films deposited by sol–gel spin coating method,” *Microscopy Research and Technique*, vol. 85, no. 4, pp. 1213-1223, 2021.
- [22] M. Arshad, M. M. Ansari, A. S. Ahmed, P. Tripathi, S. S. Z. Ashraf, A. H. Naqvi, A. Azam, “Band gap engineering and enhanced photoluminescence of Mg doped ZnO nanoparticles synthesized by wet chemical route,” *Journal of Luminescence*, vol. 161, pp. 275–280, 2015.
- [23] Y. Bouachiba, A. Mammeri, A. Bouabellou, O. Rabia, S. Saidi, A. Taabouche, B. Rahal, L. Benharrat, H. Serrar, M. Boudissa, “Optoelectronic and birefringence properties of weakly Mg-doped ZnO thin films prepared by spray pyrolysis,” *Journal of Materials Science: Materials in Electronics*, vol. 33, no. 9, pp. 6689–6699, 2022.
- [24] M. Rouchdi, E. Salmani, B. Fares, N. Hassanain, A. Mzerd, “Synthesis and characteristics of Mg doped ZnO thin films: Experimental and ab-initio study,” *Results in Physics*, vol. 7, pp. 620–627, 2017.
- [25] J. Varghese, S. K. Saji, N. R. Aswathy, R. Vinodkumar, “Influence of Mg doping on structural, optical and dielectric properties of sol–gel spin coated ZnO thin films,” *The European Physical Journal Plus*, vol. 136, no. 12, pp. 1206, 2021.
- [26] K. Upadhya U. G. Deekshitha, A. Antony, A. Ani, I. V. Kityk, J. Jedryka, A. Wojciechowski, K. Ozga, P. Poornesh, S. D. Kulkarni, N. Andrushchak, “Second and third harmonic nonlinear optical process in spray pyrolysed Mg:ZnO thin films,” *Optical Materials*, vol. 102, pp. 109814, 2020.
- [27] R. Kara, L. Mentar, A. Azizi, “Synthesis and characterization of Mg-doped ZnO thin-films electrochemically grown on FTO substrates for optoelectronic applications,” *RSC Advances*, vol. 10, no. 66, pp. 40467-40479, 2020.
- [28] F. Hussain, M. Imran, R. M. A. Khalil N. A. Niaz, A. M. Rana, M. A. Sattar, M. Ismail, A. Majid, S. Kim, F. Iqbal, M. A. Javid, S. Saeed, A. Sattar, “An

- insight of Mg doped ZnO thin films: A comparative experimental and first-principle investigations,” *Physica E: Low-dimensional Systems and Nanostructures*, vol. 115, pp. 113658, 2020.
- [29] A. Goktas, A. Tumbul, Z. Aba, M. Durgun, “Mg doping levels and annealing temperature induced structural, optical and electrical properties of highly c-axis oriented ZnO:Mg thin films and Al/ZnO:Mg/p-Si/Al heterojunction diode,” *Thin Solid Films*, vol. 680, pp. 20–30, 2019.
- [30] J. Singh, P. Kumar, K. S. Hui, K. N. Hui, K. Ramam, R. S. Tiwaria, O. N. Srivastava, “Synthesis, band-gap tuning, structural and optical investigations of Mg doped ZnO nanowires,” *CrystEngComm*, vol. 14, no. 18, pp. 5898, 2012.
- [31] D. İskenderoğlu, A. E. Kasapoğlu, E. Gür, “Valance band properties of MgZnO thin films with increasing Mg content; phase separation effects,” *Materials Research Express*, vol. 6, no. 3, pp. 036402, 2018.
- [32] P. Sahoo, A. Sharma, S. Padhan, R. Thangavel, “Visible light driven photosplitting of water using one dimensional Mg doped ZnO nanorod arrays,” *International Journal of Hydrogen Energy*, vol. 45, no. 43, pp. 22576–22588, 2020.
- [33] V. Etacheri, R. Roshan, V. Kumar, “Mg-Doped ZnO Nanoparticles for Efficient Sunlight-Driven Photocatalysis,” *ACS Applied Materials and Interfaces*, vol. 4, no. 5, pp. 2717–2725, 2012.
- [34] H. Zhuang, J. Wang, H. Liu, J. Li, P. Xu, “Structural and Optical Properties of ZnO Nanowires Doped with Magnesium,” *Acta Physica Polonica A*, vol. 119, no. 6, pp. 819–823, 2011.
- [35] S. H. Jeong, J. H. Park, B. T. Lee, “Effects of Mg doping rate on physical properties of Mg and Al co-doped Zn<sub>1-0.02</sub>Mg Al<sub>0.02</sub>O transparent conducting oxide films prepared by rf magnetron sputtering,” *Journal of Alloys Compounds*, vol. 617, pp. 180–184, 2014.
- [36] H. S. So, S. Bin Hwang, D. H. Jung, H. Lee, “Optical and electrical properties of Sn-doped ZnO thin films studied via spectroscopic ellipsometry and hall effect measurements,” *Journal of the Korean Physical Society*, vol. 70, no. 7, pp. 706–713, 2017.
- [37] S. K. O’Leary, S. Zukotynski, J. M. Perz, “Disorder and optical absorption in amorphous silicon and amorphous germanium,” *Journal of Non-Crystalline Solids*, vol. 210, no. 2–3, pp. 249–253, 1997.
- [38] F. Z. Bedia, A. Bedia, M. Aillerie, N. Maloufi, B. Benyoucef, “Structural, Optical and Electrical Properties of Sn-doped Zinc Oxide Transparent Films Interesting for Organic Solar Cells (OSCs),” *Energy Procedia*, vol. 74, pp. 539–546, 2015.
- [39] K. Huang Z. Tang, L. Zhang, J. Yu, J. Lv, X. Liu, F. Liu, “Preparation and characterization of Mg-doped ZnO thin films by sol–gel method,” *Applied Surface Science*, vol. 258, no. 8, pp. 3710–3713, 2012.
- [40] B. Kim, D. Lee, B. Hwang, D.-J. Kim, C. K. Kim, “Effects of Mg doping and annealing temperature on the performance of Mg-doped ZnO nanoparticle thin-film transistors,” *Molecular Crystals and Liquid Crystals*, vol. 235, no.1, pp. 61–74, 2021.
- [41] M. Caglar, Y. Caglar, S. Ilcan,

- “Investigation of the effect of Mg doping for improvements of optical and electrical properties,” *Physica B: Condensed Matter*, vol. 485, pp. 6–13, 2016.
- [42] B. H. Kim, C. M. Staller, S. H. Cho, S. Heo, C. E. Garrison, J. Kim, D. J. Milliron, “High Mobility in Nanocrystal-Based Transparent Conducting Oxide Thin Films,” *ACS Nano*, vol. 12, no. 4, pp. 3200–3208, 2018.
- [43] L. T. C. Tuyen, S.-R. Jian, N. T. Tien, P. H. Le, “Nanomechanical and Material Properties of Fluorine-Doped Tin Oxide Thin Films Prepared by Ultrasonic Spray Pyrolysis: Effects of F-Doping,” *Materials (Basel)*, vol. 12, no. 10, pp. 1665, 2019.
- [44] P. Senthilkumar, S. Raja, R. Ramesh Babu, G. Vasuki, “Enhanced electrical and optoelectronic properties of W doped SnO<sub>2</sub> thin films,” *Optical Materials*, vol. 126, pp. 112234, 2022.
- [45] G. Turgut, E. F. Keskenler, S. Aydın, D. Tatar, E. Sonmez, S. Dogan, B. Duzgun, “Characteristic evaluation on spray-deposited WFTO thin films as a function of W doping ratio,” *Rare Metals*, vol. 33, no. 4, pp. 433–441, 2014.
- [46] E. Vinoth, S. Gowrishankar, N. Gopalakrishnan, “Effect of Mg doping in the gas-sensing performance of RF-sputtered ZnO thin films,” *Applied Physics A*, vol. 124, no. 6, p. 433, 2018.